ISBN: 978-3-95450-200-4 doi:10.18429/JACoW-ICAP2018-MOPAF02

REALISTIC MODELING OF THE MUON $g-2$ EXPERIMENT BEAMLINES AT FERMILAB*

D. A. Tarazona†, M. Berz, K. Makino, Michigan State University, East Lansing, MI, USA
D. Stratakis, M. J. Syphers[1], Fermi National Accelerator Laboratory, Batavia, IL, USA
[1]also at Northern Illinois University, DeKalb, IL, USA

Abstract

The main goal of the Muon $g-2$ Experiment at Fermilab (E989) is to measure the muon anomalous magnetic moment (a_μ, also dubbed as the "anomaly") to unprecedented precision. This new measurement will allow to test the completeness of the Standard Model (SM) and to validate other theoretical models beyond the SM. Simulations of the beamlines from the pion production target to the entrance of the $g-2$ Storage Ring (SR) using COSY INFINITY [1] contribute to the understanding and characterization of the muon beam production in relation to the statistical and systematic uncertainties of the E989 measurement. The effect of nonlinearites from fringe fields and high-order contributions on the beam delivery system performance are considered, as well as interactions with the beamline elements apertures, particle decay channels, spin dynamics, and beamline misalignments.

INTRODUCTION

The most recent measurement of a_μ at the Brookhaven National Laboratory Muon $g-2$ Experiment (E821) yielded an experimental relative uncertainty of 0.54 ppm, which differs from current SM predictions by about 3.7σ [2]. In contrast to E821, the goal of E989 is to deliver a measurement of the anomaly to a precision of 0.14 ppm or less to reach $> 5\sigma$ discrepancy with the SM and therefore strongly establish evidence for new physics.

For that purpose, the number of recorded muon decays in the $g-2$ storage ring at E989 is required to increase by a factor of 20 with respect to E821. The Fermilab Muon Campus E989 beam delivery system (BDS), which is a set of 1 km-long beamlines between the pion-production target and the entrance of the storage ring downstream, is designed to meet the statistical goal and deliver $(0.5\text{–}1.0)\times10^5$ muons to the storage ring per 10^{12} protons interacting with the pion-production target.

On the other hand, the relative statistical uncertainty in the experimental a_μ is inversely proportional to the muon beam polarization (see [2], Eq. (16.6)). Thus, it is worth to study the effect of nonlinearities and perform spin dynamics simulations. In addition, due to the momentum acceptance of about ±0.5% of the storage ring it is of interest to numerically evaluate the dynamical properties of the muon beam as it is delivered to the muon storage ring.

Motivated by the reasons exposed above, we have developed a model of the E989 beamlines to reproduce numerical simulations of the muon beam's statistical performance and dynamical behavior including spin using COSY INFINITY. This program prepares detailed high-order transfer maps calculated with an 8th order Runge-Kutta integrator and Differential-Algebraic (DA) methods to solve the beam optics Ordinary Differential Equations (ODEs) and perform beam tracking. In particular, we present results from tracking of secondary protons, pions, daughter muons from pion decay, and muons produced right at the entrance of the E989 beamlines downstream the pion-production target. Nonlinear effects due to standard fringe fields, up to 4th-order beam dynamics, spin dynamics, beam collimation, and misalignments of the multiple BDS beamline elements are considered.

The paper begins with a brief description of the Muon Campus E989 beam delivery system. Then details of the beam dynamics simulations throughout the E989 beamlines from the production target to the storage ring entrance and beam performance results considering nonlinear effects are discussed.

E989 BEAM DELIVERY SYSTEM (BDS)

The main purpose of the E989 beamlines considered in simulations, depicted in Figure 1, is to deliver a clean muon beam with momentum $p_0 = 3094\,\text{MeV}/c$ to the storage ring. Batches of four bunches made of 10^{12} protons each are directed to an Inconel-600 "pion-production" target located at the AP0 target hall, from which positive secondary particles emerge. 30 cm downstream the target, a 232 T/m magnetic gradient produced by a lithium lens focuses the secondaries. Thereafter, a pulsed magnet with a field of 0.53 T selects $3.115\,\text{GeV}/c$ ±10% positive particles and bends them 3° towards the 50 m long M2 line, which consists of matching quadrupoles followed by eight more quadrupoles and a dipole that horizontally bends the beam 3° to match with the M3 line (230 m long).

The M3 line is made of FODO cells that maintain small beta functions to provide continuity of pions and daughter muons from pion decay. By the end of M3, the secondary beam is mainly composed of protons that do not interact with the target, pions that need more time to decay, and muons. In order for such beam to become a clean muon beam, the M3 line is aligned with the injection leg of the Delivery Ring (DR) for which horizontal bends deviate the beam to the right by about 18° at $s \sim 160$ m away from the target (s represents the longitudinal distance). At the end of M3, a series of magnets involving a C-magnet, a pulsed magnetic

* Fermilab report: FERMILAB-CONF-18-620-APC.
† Email: tarazona@msu.edu. ORCID: 0000-0002-7823-7986.

This manuscript has been authored by Fermi Research Alliance, LLC under Contract No. DE-AC02-07CH11359 with the U.S. Department of Energy, Office of Science, Office of High Energy Physics.

ISBN: 978-3-95450-200-4 doi:10.18429/JACoW-ICAP2018-MOPAF02

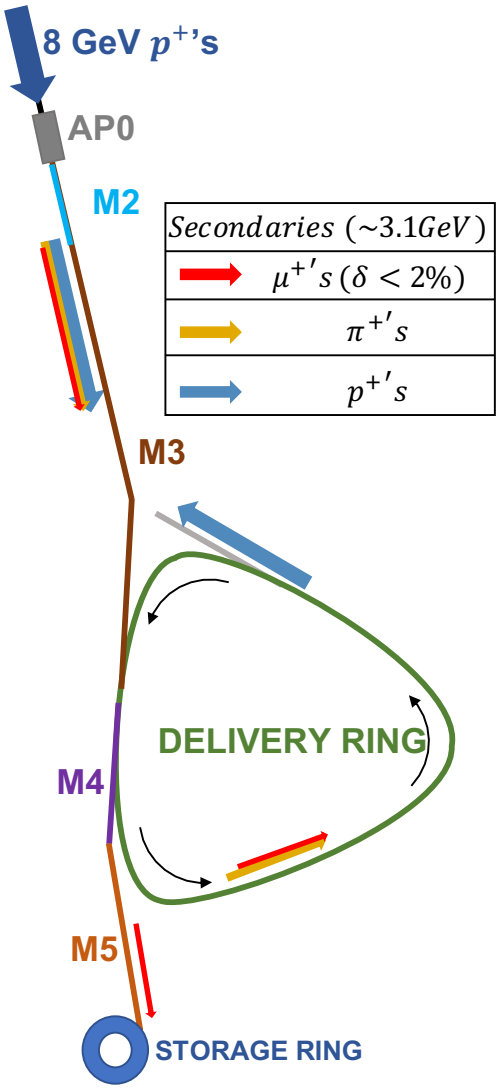

Figure 1: A schematic layout of the BDS.

septum dipole, and kicker modules inject the beam DR after a vertically upward bend of about 5.7°.

Through the 505 m of circumference of the DR, previously used as a debuncher ring and now reconditioned for E989, the remaining pions have enough time to decay into mostly muons as they circulate four times before being extracted into the M4 line. The DR also allows protons to spatially separate from the other lighter particles by a rate of 75 ns per turn [3]; this feature lets a kicker within the DR to safely remove the protons after the fourth turn. The optics functions of the DR using COSY are shown in Fig. 2.

The resulting muon beam is then extracted to the multiple vertical bends and quads of the M4 beamline (30 m), followed by the M5 line (100 m) with a tunable final focus section and ultimately be delivered into the entrance of the storage ring.

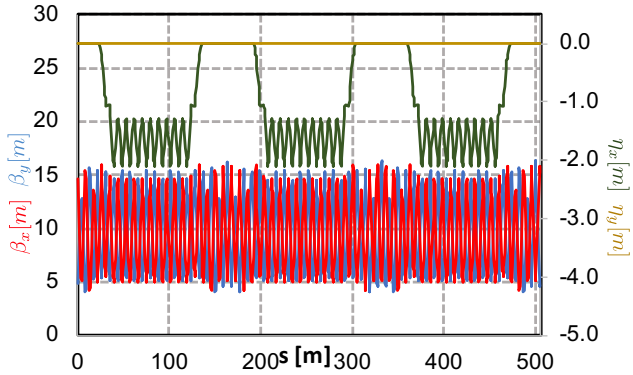

Figure 2: DR optics functions. Fringe fields considered in simulations change the beta functions by less than 3%. The dispersion horizontal function (η_x) reveals the three-fold symmetry of the ring. Optics functions have served as a channel to validate our BDS model.

SIMULATION DETAILS AND RESULTS

The following results have served to benchmark other numerical studies at E989 modeled with G4Beamline [3] and Bmad [4]. Moreover, the inclusion into our model of nonlinearities from fringe fields and high-order effects and an analysis covering various misalignment scenarios provide further realism to the characterization of the muon beam that is delivered to the storage ring.

Tracking simulations of the E989 beamlines start with a 6D initial distribution at the exit of the pion-production target from a modeling with MARS [5] of 10^9 protons on target. We consider protons, muons, and pions, although other particles emerge from the target as verified by experimental evidence though at significantly smaller ratios [6].

The presented studies consider aperture beam collimation. There are several aperture geometries determined by the multiple purposes of the elements in the E989 beamlines as well as the expected beam size behavior from design. They range from simple squared and circular apertures to more involved star-shaped apertures which can be approximated as an overlaying of ellipses and rectangles in COSY. In simulations, particles are removed from the beam if their spatial transversal coordinates surpass the dimensions of the aperture. This algorithm is repeated every 20 cm or so, depending on the beamline longitudinal size. COSY permits to track 10,000 particles simultaneously, which reduces the computational time. In this manner, the statistical performance of the beam and resulting beam dynamics variables distributions are determined.

Figure 3 shows the number of secondaries throughout the M2 and M3 lines after the production target. At the end of these lines about 10^{-4} protons per proton on target (POT) remain within the secondary beam, which are kicked out downstream at the Delivery Ring. The in-flight decay channels considered in simulations are $\pi^+ \rightarrow \mu^+ + \nu_\mu$ and $\mu^+ \rightarrow e^+ + \nu_e + \bar{\nu}_\mu$. The effect of muon decays on the

ISBN: 978-3-95450-200-4 doi:10.18429/JACoW-ICAP2018-MOPAF02

overall number of muons throughout the beamlines is not significant due to the short time it takes for the beam to travel from the production target to the entrance of the storage ring, i.e. 8.1 µs. Since the momentum admittance at the storage ring is ±0.5%, we track muons within specific momentum offsets (δ) as shown in Fig. 3.

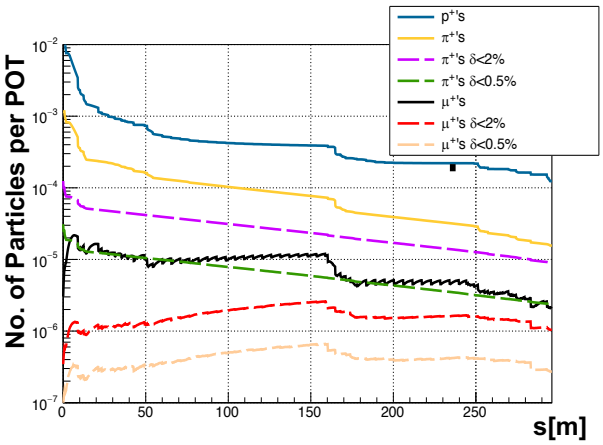

Figure 3: Statistical performance along M2/M3.

The range $|\delta| < 2\%$ is considered as well in connection with upcoming efforts at E989 to manipulate the beam momentum range with wedge cooling [7]. As shown in Fig. 3, M2/M3 lines maintain the statistics of muons with $|\delta| < 2\%$ emerging from pion decay. Main muon losses of about 11% and 20% take place at the 18.5° horizontal bend ($s \sim 160.0$ m) and along the vertical injection upstream the DR ($s \sim 280.0$ m), respectively. The black dot around $s \sim 235$ m in Fig. 3 depicts the number of total particles per POT from measurements, suggesting reliability on our simulations results. Aperture beam collimation allows to predict the final beam momentum distribution at the entrance of the SR, shown in Fig. 4. Similar simulations were performed along the rest of the E989 beamlines downstream M3 (results are summarized in Table 1).

Table 1: Statistical Performance Along BDS [POT]

	M3 exit	DR exit ($n = 4$)	SR entrance
μ's	2.19×10^{-6}	1.04×10^{-6}	7.48×10^{-7}
μ's*	2.72×10^{-7}	2.85×10^{-7}	1.89×10^{-7}
π's	1.55×10^{-5}	0	0
p's**	1.24×10^{-4}	6.80×10^{-5}	5.86×10^{-5}

*Results for $\delta < 0.5\%$
**Results for the case of proton removal at DR turned off.

Fringe fields map computations are performed at the edges of each beamline element. The longitudinal-dependent tapering of the multipole strengths is modeled by a six parameter Enge function:

$$F(z) = \frac{1}{1 + \exp\left(a_1 + a_2 \cdot (z/D) + \cdots + a_6 \cdot (z/D)^5\right)},$$

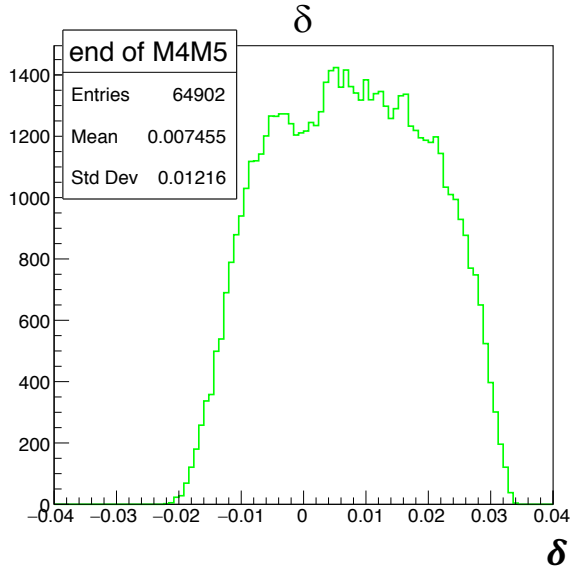

Figure 4: Beam relative momentum distribution at the storage ring entrance.

where z is the distance perpendicular to the effective field boundary and D is the full aperture of the particle optical element. The a_i coefficients are taken by default based on measured data from PEP at SLAC [8]; for such cases, the integrated multipole strengths along the optical axis of each beamline element remain the same as for simulations with hard-edge modeling. Therefore, the following comparisons between numerical results with fringe field effects turned on and off are reliable.

4th-order numerical calculations with and without fringe fields were implemented. Figure 5 shows the differences between the two scenarios along the DR.

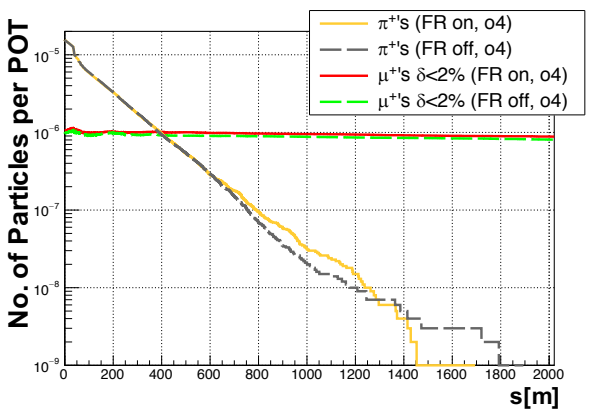

Figure 5: Fringe field effects on beam population at the DR.

After four turns, simulations suggest a favorable contribution due to fringe fields on the muons (i.e. 9.4% increment) and pions population. Fringe fields introduce fields longitudinal to the beam motion, which may be the essential contributor to keep more particles focused in a similar way

ISBN: 978-3-95450-200-4 doi:10.18429/JACoW-ICAP2018-MOPAF02

to solenoids for low-energy experiments. However, such effect is not sufficiently large to compensate for losses at the beam bends along the Beam Delivery System in a significant way. Specifically, simulation results show an increment of 5.2% more muons at the entrance of the storage ring. Moreover, fringe fields have a larger contribution in the number of surviving muons than in pions; i.e. at the end of the M3 line (s = 290 m) —where most of pions still have not decayed—fringe fields maintained 8.9% more muons on track whereas pions population increment at that location increased by only 0.4%, which is within the ~2% range of the simulations' statistical error.

On the other hand, fringe fields from the BDS beamline elements were also considered in spin tracking simulations. For the pion decay channel, the resulting muon beam polarization is calculated based on a module that considers the weak interaction process to get the direction of the muon spin vector [9] and tracked with COSY's DA mapping calculation [8]. In Fig. 6, the spin components of a beam made of 64,902 muons at the entrance of the SR are plotted from simulations.

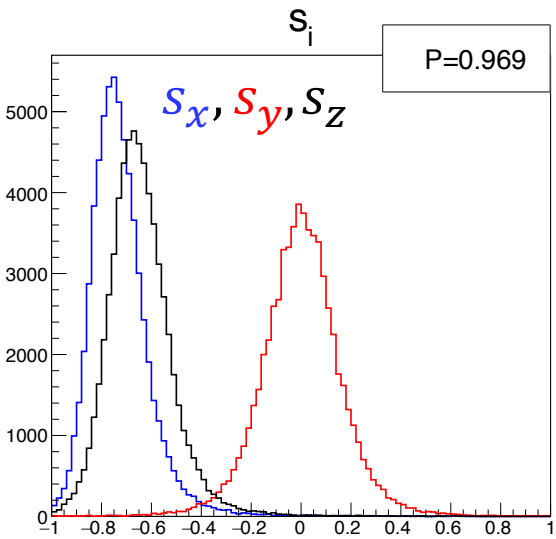

Figure 6: Muon beam spin components at SR entrance.

The components are expressed in terms of the coordinates that describe the relative dynamics around the reference orbit [10]. The resulting polarization is P = 0.97, in agreement with G4Beamline numerical simulations [3] which do not consider fringe fields. Thus, fringe fields do not interfere with the muon beam polarization. Another spin variable worth to consider is the polarization projection in the horizontal plane with respect to the reference optical axis, φ_a (see Fig. 7). The precession frequency of this phase, ω_a, plays an essential role in the final measurement of a_μ^{E989} which implies a deep understanding of its evolution as the beam circulates through the SR. In particular, the correlation between φ_a and the Lorentz factor γ of a muon results in a sub-ppm systematic effect of ω_a; high-momentum muons decay rate is slower than low-momentum muons and consequently ω_a shifts as the muon beam decays [11].

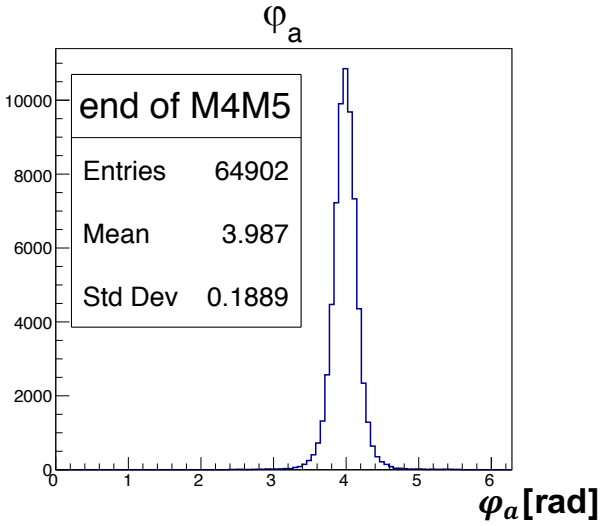

Figure 7: φ_a at SR entrance.

Tracking simulations were performed with and without fringe fields to study the effect of fringe fields on the spin-momentum correlation $m_\delta = d\langle\varphi_a\rangle/d\gamma$. For the case of fringe fields turned on, simulations show a correlation m_δ equal to 29.2±9.4 mrad after 4 turns around the DR as shown in Fig. 8. On the other hand, similar simulations without fringe fields —conventional hard-edge model— indicate a correlation m_δ = 92.1 ± 9.8 mrad. Thus, our numerical studies suggest a significant effect of fringe fields on spin-momentum correlations.

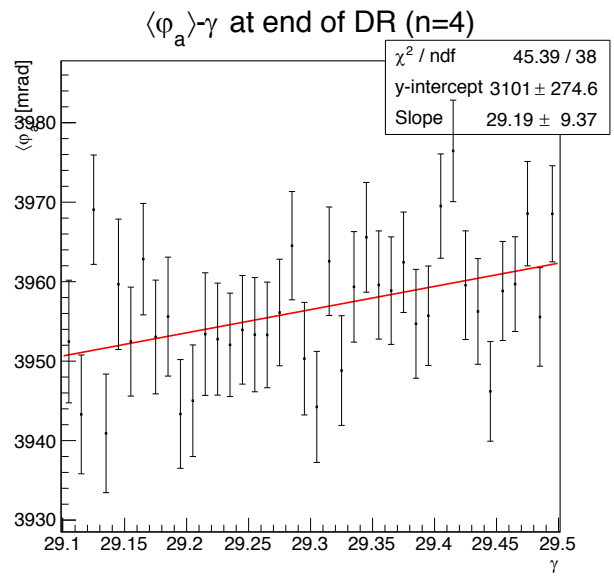

Figure 8: $\langle\varphi_a\rangle$ vs. γ at DR exit after 4 turns.

Misalignments are introduced in simulations by transforming the transport maps that represent each beamline element.

ISBN: 978-3-95450-200-4 doi:10.18429/JACoW-ICAP2018-MOPAF02

Transformations follow randomly Gaussian-distributed horizontal and vertical misplacements with standard deviations of 0.25 mm, introducing constant terms to the maps. A total of ten random misalignment configurations of the beam delivery system initialized with different random seeds were considered to procure statistical ranges within which the beam performance would be expected to occupy.

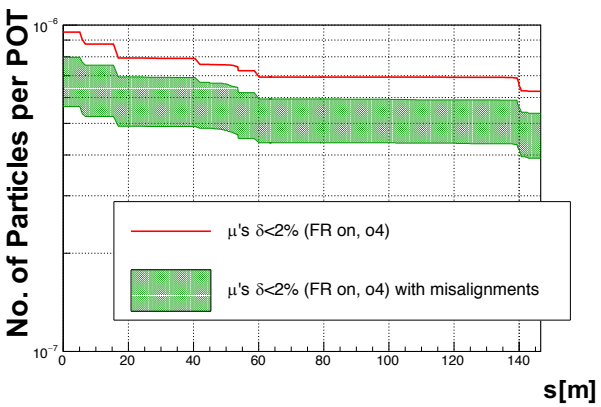

Figure 9: Misalignment effects on beam population at M4/M5 lines.

Figure 9 shows how the misalignments under consideration could decrease the number of muons that make it to the end of M5. However, even though 0.25 mm is a small RMS, the correctors along the beamlines are expected to reduce such detrimental effect.

In addition to the linear description of the beam dynamics, COSY INFINITY allows the computation of higher order effects of the beamline elements [8]. In specific, particle coordinates as defined in COSY are calculated as follows:

$$r_i = \sum_{l_1,l_2,\ldots,l_6=0}^{\leq 4} (r_i|x^{l_1}a^{l_2}y^{l_3}b^{l_4}l^{l_5}\delta^{l_6})x_0^{l_1}a_0^{l_2}y_0^{l_3}b_0^{l_4}l_0^{l_5}\delta^{l_6}$$

where the expression in parenthesis indicates the corresponding transport map component, up to fourth-order in our simulations.

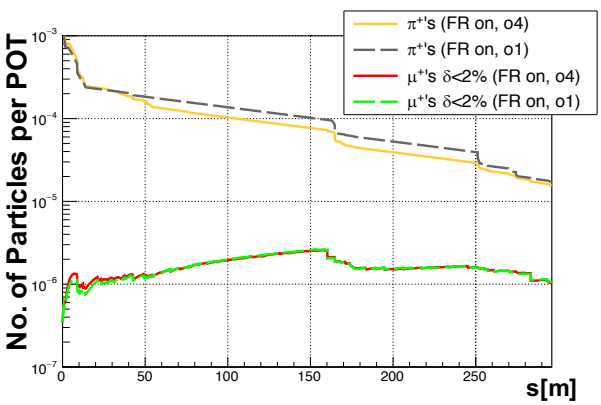

Figure 10: High-order effects on beam population at M2/M3 lines.

As shown in Fig. 10, high-order components seem not to change the statistical performance of the beam.

CONCLUSION

A detailed model of the Beam Delivery System at E989 has been developed using COSY INFINITY. Realistic features based on DA methods, such as fringe fields, high-order effects, and misalignments are included to describe the statistical and dynamical performance of the secondary beam produced at the pion-production target. Simulation results suggest that fringe fields increase the number of muons that are delivered to the storage ring by ∼5%, whereas the muon beam polarization is unaffected. However, spin-momentum correlations that could add systematic effects to the final measurement of E989 due to differential decays are significantly affected by the fringe fields from the rectangular magnets of the delivery ring. High-order effects do not affect the secondary beam performance and misalignments without correctors were also considered in simulations. Our simulations also served to validate numerical calculations prepared by other members of the Muon $g-2$ Collaboration and check the performance of the BDS.

ACKNOWLEDGEMENTS

We are thankful to the Muon g-2 Collaboration at Fermilab, specially W.M. Morse, J.P. Morgan, M. Korostelev, and V. Tishchenko for all the discussions and suggestions. This work was supported by the U.S. Department of Energy under Contract No. DE-FG02-08ER41546. This manuscript has been authored by Fermi Research Alliance, LLC under Contract No. DE-AC02-07CH11359 with the U.S. Department of Energy, Office of Science, Office of High Energy Physics. We are grateful to the PhD Accelerator Program at Fermilab and also for a Strategic Partnership Grant from the MSU Foundation.

REFERENCES

[1] K. Makino and M. Berz, "COSY INFINITY Version 9", *Nucl. Instr. Meth. A*, vol. 558, pp. 346–350, 2006.

[2] J. Grange *et al.*, "Muon g–2 Technical Design Report", Fermi National Accelerator Laboratory, Batavia, IL, USA, FERMILAB-FN-0992-E, Jan. 2015.

[3] D. Stratakis, M. E. Convery, C. Johnstone, J. Johnstone, J. P. Morgan, D. Still, J. D. Crnkovic, V. Tishchenko, W. M. Morse, and M. J. Syphers, " Accelerator performance analysis of the Fermilab muon campus", *Phys. Rev. Accel. Beams*, vol. 20, pp. 111003, Nov 2017.

[4] M. Korostelev *et al.,* "End-to-end beam simulations for the new muon g-2 experiment at Fermilab," in *Proc. IPAC'16*, Busan Korea, May 2016. doi:10.18429/JACoW-IPAC2016-WEPMW001

[5] MARS, http://mars.fnal.gov

[6] D. Stratakis, "Recent Results from the Muon Campus runs", $g-2$ Experiment Document GM2-doc-13633, Muon $g-2$ Collaboration, Fermi National Accelerator Laboratory, Batavia, IL, USA, 2018.

ISBN: 978-3-95450-200-4 doi:10.18429/JACoW-ICAP2018-MOPAF02

[7] D. Stratakis, "Recent Results from the Muon Campus runs", $g-2$ Experiment Document GM2-doc-11124, Muon g-2 Collaboration, Fermi National Accelerator Laboratory, Batavia, IL, USA, 2018.

[8] M. Berz and K. Makino, "COSY INFINITY 10.0 Beam Physics Manual", Department of Physics and Astronomy, Michigan State University, East Lansing, MI, USA, Rep. MSUHEP-151103, Oct 2017.

[9] F. Combley and E. Picasso, The muon (g-2) precession experiments: Past present and future, *Phys. Rep.* 14, 1 (1974).

[10] M. Berz, K. Makino, and W. Wan, *An Introduction to Beam Physics*, CRC Press, Boca Raton, FL, USA 2016.

[11] J. Crnkovic *et al.*, "Spin Correlations study for the new $g-2$ Experiment at Fermilab," in *Proc. IPAC'16*, Busan Korea, May 2016. doi:10.18429/JACoW-IPAC2016-TUPMR028